sustainability

MDPI

Article

Assessing the Future Water and Energy Security of a Regulated River Basin with a Coupled Land Surface and Hydrologic Model

Jing Xiao [1,2] and Ningpeng Dong [1,3,*]

1 Key Laboratory of Flood & Drought Disaster Defense, the Ministry of Water Resources, Nanjing 210029, China
2 Hydrology and Water Resources Survey Bureau of Hainan Province, Haikou 570100, China
3 State Key Laboratory of Simulation and Regulation of Water Cycle in River Basin, China Institute of Water Resources and Hydropower Research, Beijing 100038, China
* Correspondence: dongnp@iwhr.com

Abstract: To address the water-related issues faced by humans, the planning and construction of dams, water diversion projects, and other water infrastructures have been continuously adopted by decision makers worldwide. This is especially the case for the Yalong River Basin (YRB) in China, which is expected to be one of the most regulated rivers due to reservoir construction and the planned South-to-North Water Diversion project. To understand the potential impact of these water infrastructures on the water resources and hydropower production of the basin and downstream areas, we employ a land surface–hydrologic model with explicit representations of dam operation and water diversions in order to quantify the impact of reservoir operation and water diversion on the future water and energy security of the YRB. In particular, a conceptual reservoir operation scheme and a hydropower-optimized reservoir operation scheme are employed to predict the future release, storage and hydropower generation of the YRB, respectively. Results indicate that reservoirs can have noticeable, cumulative effects in enhancing the water security by reducing the wet season streamflow by 19% and increasing the dry season streamflow by 66%. The water diversion can result in an overall decrease in the streamflow, while the downstream reservoirs are expected to fully mitigate the decline in the dry season streamflow. The hydropower production is likely to decrease by 16% and 10% with conventional and optimized operation schemes, respectively, which suggests that the adaptation of operation rules alone cannot reverse the decline in the electricity production. Our findings can provide implications for sustainable water resource management.

Keywords: dam operation; energy security; land surface–hydrologic modeling; water security; water diversion

Citation: Xiao, J.; Dong, N. Assessing the Future Water and Energy Security of a Regulated River Basin with a Coupled Land Surface and Hydrologic Model. *Sustainability* **2023**, *15*, 4106. https://doi.org/10.3390/su15054106

Academic Editor: Fernando António Leal Pacheco

Received: 27 January 2023
Revised: 19 February 2023
Accepted: 21 February 2023
Published: 24 February 2023

1. Introduction

Population growth has led to increasing water demand and energy consumption during the past few decades, which will continue to pose large challenges for the sustainability of social-economic development in the future in the context of the warming climate [1]. To alleviate the water and energy shortages that are likely to become worse in the near future, dams and other water infrastructures have been widely built by decision makers across the globe [2,3]. Currently, the total amount of water stored in reservoirs has reached a point that is around three times higher than the annual mean water stored in global river channels [4]; in addition, the global hydroelectricity generation tripled during the period of 1973–2016 [5].

Typically, explicitly incorporating human activities into hydrologic models is adopted to assess the impact of water infrastructure on changes in hydrological, biological, and ecological conditions [6–10]. These include representations of reservoirs, water abstractions, and irrigation practices over different spatiotemporal scales [11–13]. Much of the existing literature working on climate change impact mitigation has employed hydrologic modelling to formulate and evaluate possible mitigation strategies; this includes reservoir operation, in order to mitigate risks such as flooding and irrigation failure in watersheds in different climatic regions [3,14]. Recent studies have also made progress in extending traditional hydrological models, for example, by coupling hydrological processes with thermodynamic processes [15] and surface hydrodynamics [16].

Despite the importance of explicitly parameterizing anthropogenic disturbance in hydrologic models, uncertainties still exist in modeling estimates [17–19]. While many modeling studies have developed reservoir operation schemes in hydrologic models to account for reservoir impacts, many of these schemes more or less require historic reservoir operation data (inflow, outflow, storage, etc.) in order to derive the reservoir outflow, which are often not available at regional scales and limit the applicability of these schemes [20–22]. In addition, many of the above-mentioned studies have only considered the parameterization of a single human activity, yet ignored the mutual interaction between multiple human activities, for example, reservoir operation and water diversions. This could lead to errors in estimating the regional water and energy security [23,24].

With the ongoing development of water infrastructures, the Yalong River Basin (YRB) in China will likely be regulated by a dozen hydropower reservoirs and the South-to-North Water Diversion project in the future. In this context, the water security and energy security of the basin and areas further downstream has raised nationwide concern. On one hand, the YRB is the third largest hydropower base in the country. It plays an important role in guaranteeing the water and energy security in Southwest China [25,26]. On the other hand, several water infrastructures are being planned in the basin in order to address the scarcity of water resources and electricity outside the basin. For example, a long-term, large-scale water division project, i.e., the western route of SNWD, has been recently promoted to transport water from the Yangtze River basin to the Yellow River basin (i.e., the second-longest river in China) and, eventually, mitigate drought risks in the Yellow River basin. In addition to the western route of SNWD, several large-sized hydropower reservoirs have been under construction and planning for exploring hydropower potential, which corresponds to the largest reservoir building agenda in China [27].

In this study, we aim to assess the cumulative impacts of dam construction and water diversion on the regional water security and energy security of the YRB in a quantitative manner. To this end, we employ a coupled land surface–hydrologic model (CLHMS), coupled with a conceptual reservoir operation scheme, in order to simulate the release and hydropower production of the major reservoirs in the YRB. A water diversion parameterization is also implemented in the reservoir operation scheme to represent the water diversion processes. To investigate the most favorable energy security condition of the YRB in the future, a hydropower optimization scheme is implemented into the CLHMS model to calculate the maximum possible hydropower generation of the reservoirs in the YRB.

2. Data and Methods

2.1. Study Area

The Yalong River Basin (YRB) is located in the upper Yangtze River Basin, with an area of 13.6×10^4 km^2 (Figure 1). The basin lies on the eastern edge of the Tibetan Plateau and is characterized by plateau climate, rugged terrain and a sparse population. The average annual precipitation of the basin is approximately 800 mm, and nearly 80% occurs between June and October, dividing a year into the wet season and dry season. The Ertan station, located immediately upstream of the Ertan Reservoir, is often considered the controlling hydrologic station of the basin.

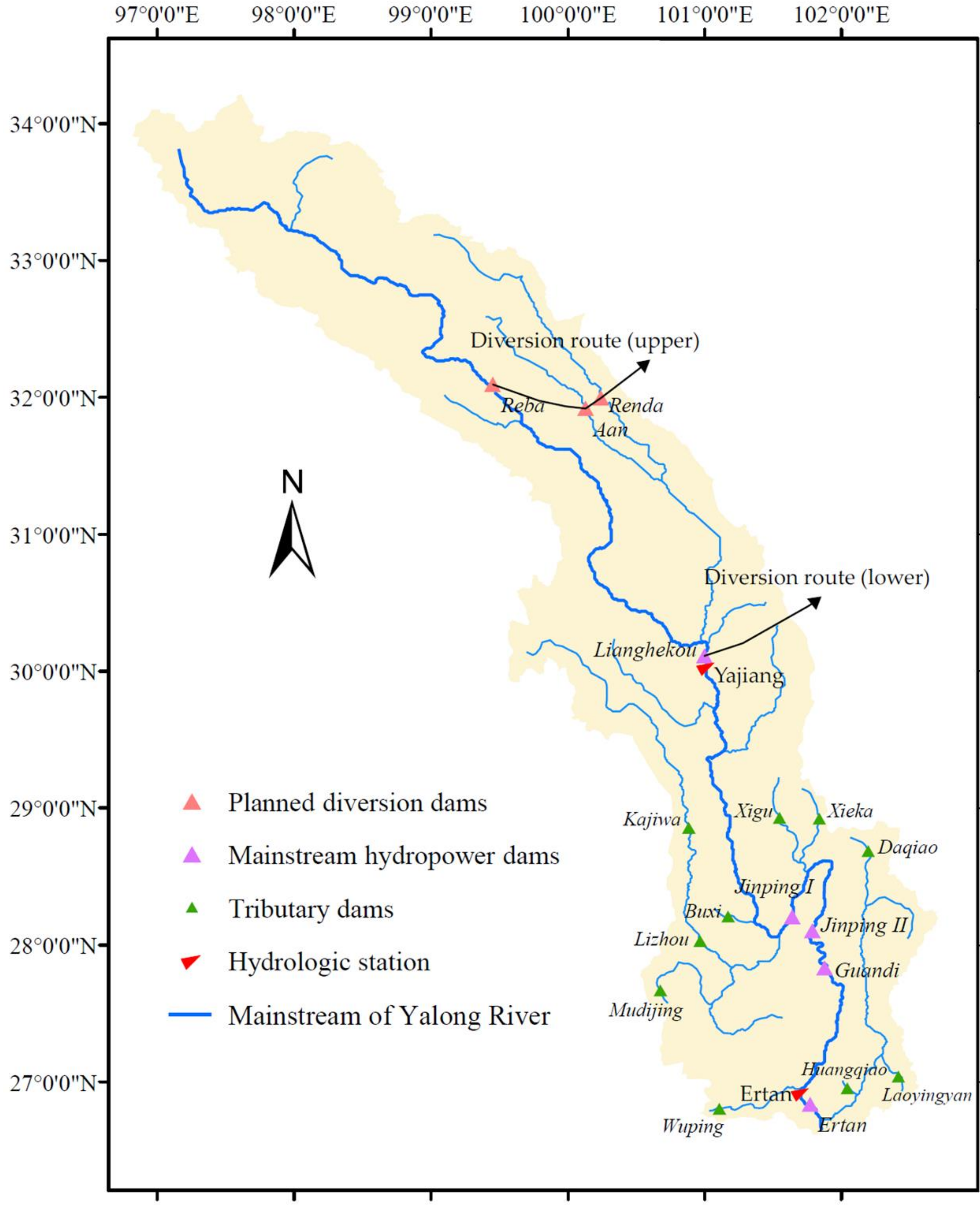

Figure 1. The water diversions and reservoirs in the Yalong River Basin. The black lines and arrows represent the water diversion routes and its directions.

As of 2021, there are five large hydropower reservoirs in the mainstream, and a dozen more under construction and planning. Out of the five mainstream hydropower reservoirs, three have a massive capacity to regulate the streamflow, namely Lianghekou (capacity: 1.2×10^{10} m^3, nearly completed but not fully operational until 2024), Jinping I (capacity: 8.0×10^9 m^3, fully operation since 2014) and Ertan (capacity: 6.1×10^9 m^3, fully operational since 1998). The remaining two mainstream hydropower reservoirs, namely Jinping II and Guandi, and the other planned hydropower reservoirs, generally release the water directly on a daily scale without any regulation due to their small capacity. In addition, there are ten tributary reservoirs with a capacity larger than 1×10^7 m^3, which may have a notable hydrological impact at the local scale and beyond. All of these tributary reservoirs were built after 2010.

The western route of the South-to-North water diversion is intended to divert billions of cubic meters of water from the YRB to the Yellow River Basin. The latest diversion scheme was proposed and approved by the Ministry of Water Resources in 2020, which consists of the upper route and the lower route [27]. For the upper route, three diversion reservoirs, namely Reba, Ana and Renda, will be built for water abstraction, with 2.85 billion m^3 of water to be diverted per year. For the lower route, 4 billion m^3 of water will be abstracted and diverted from the Lianghekou reservoir per year. The monthly diverted water was determined based on the net water demand of the upper Yellow River Basin, which was collected from the water authority of the Yellow River Basin.

2.2. The Coupled Land Surface and Hydrologic Model System CLHMS

In this study, the CLHMS, i.e., a fully coupled system of the land surface scheme of GENESIS (LSX) and the physically based Hydrological Model System (HMS) [28,29], is extended and used for our water and energy security modeling study. The LSX solves the surface runoff, soil infiltration, and evapotranspiration based on the water and energy balance on a raster grid basis; meanwhile, the HMS derives the surface water routing using the diffusive wave equation and describes the soil moisture motion using the 1D Richards equation. The model is also coupled with a 2D lake/floodplain module and a 2D groundwater routing model, which represent the surface water and groundwater dynamics, respectively.

Multiple studies using the CLHMS model have reported good agreement between the simulation and observation of multiple hydrological components, including streamflow, soil moisture, groundwater levels, and evapotranspiration [30–34]. In this study, the daily meteorological data needed to drive the CLHMS consists of the CN05.1 precipitation dataset (http://data.cma.cn, accessed on 10 December 2022) and the NCEP/NCAR reanalysis dataset (http://rda.ucar.edu/datasets, accessed on 10 December 2022). The model was run at a daily scale and at spatial resolution of 5 km (~0.045° at the equator).

2.3. Parameterization of Reservoirs and Water Diversion

The CLHMS model used in this study is coupled with a reservoir operation module. Here, the five mainstream hydropower reservoirs and ten tributary reservoirs (Section 2.1) are directly integrated into the CLHMS model via the reservoir module. The western route of the SNWD project consists of three diversion reservoirs with diversion channels, and are, therefore, also parameterized via the reservoir module. To account for the water abstracted from the reservoir for diversion, an additional water diversion term D, is introduced in the reservoir water balance equation:

$$V_t = V_{t-1} + \Delta t \cdot (I_t - Q_t + A_t \cdot P - A_t \cdot E - A_t \cdot S - D) \quad (1)$$

where V_{t-1} and V_t are the reservoir storage at the last time step and current time step; Δt is the model time step; I_t and Q_t are the inflow and the outflow of the reservoir, respectively; A_t is the water surface area at the timestep t; E is the evaporation, which is calculated with the Penman Equation; P is the precipitation on the reservoir water surface; and S is the reservoir–groundwater flux derived from the Darcy's Law.

2.3.1. Conceptual Reservoir Operation Scheme

Conceptual reservoir operation schemes have been widely used in hydrologic modelling to estimate and predict the release of reservoirs by establishing empirical functions between release, storage, inflow, and/or water demand. In this study, a conceptual reservoir operation scheme [20–22] (hereinafter 'D22') is used to approximate the reservoir releases and storages in reality. The release of reservoirs, Q_t, is calculated as follows:

$$Q_t = \begin{cases} min\left(Q_{min},\ \frac{V_t}{\Delta t}\right)\ (V_t \le V_d) \\ max(Q_{min},\ r \cdot U_t)\ (V_d < V_t \le V_c) \\ r \cdot U_t + (Q_s - r \cdot U_t) \cdot \left(\frac{V_t - V_c}{V_f - V_c}\right)^k \left(V_c < V_t \le V_f\right) \\ max\left(Q_s,\ \frac{V_t - V_f}{\Delta t}\right) \left(V_t > V_f\right) \end{cases} \quad (2)$$

where V_t, V_d, V_c and V_f refer to the reservoir storage at the timestep t, at the dead level, at the conservation level, and at the high flood level, respectively. Q_{min} is the minimum release; r is a parameter indicative of the current storage anomalies; U_t is the human water demand at the timestep t; Q_s is the maximum allowable reservoir release to protect downstream areas from flood inundation; and k ($k \le 1$) is a flood indicator equal to the ratio of Q_s to the inflow.

Among these parameters, Q_{min}, Q_s, U_t and r need to be determined according to the availability of the in situ reservoir operation data. When in situ data is not available, we determine these parameters empirically, which we denote as *empirical parameters* hereinafter. Specifically, Q_{min} and Q_s are set as the 10th and 99th percentiles of the non-exceedance probabilities of the simulated streamflow, respectively. r is derived on a daily scale based on the relative difference between the current storage V_t and the daily target storage V_{tar}, and r at the time t is expressed as follows:

$$r_t = \left(1 + c \cdot \frac{V_t - V_{tar}}{V_{cd} - V_d}\right) \quad (3)$$

with

$$c = min\left(\frac{I_a}{3 \cdot (V_{cd} - V_d)}, 1\right) \quad (4)$$

where V_{cd} is the reservoir storage at the conservation level in the dry season, which corresponds to the maximum normal operating level; V_{tar} is the daily target storages derived as the 10-day rolling mean of the multi-year median (multi-year mean) daily in situ releases and storages for within-year reservoirs (over-year reservoirs); I_a is the mean annual inflow; and c is an empirical parameter to avoid excessive release variations for over-year reservoirs.

When in situ data is available, these parameters can be derived through calibration, which we denote as *calibrated parameters*. The release thresholds Q_{min} and Q_s are calibrated directly to the reservoir operation data. With respect to the parameter r, the concept of target releases Q_{tar} is introduced to replace human water demand U_t, in order to implicitly represent the downstream water demands at different times of the year, and r can be expressed as follows:

$$r = \frac{Q_{tar}}{U_t} \cdot \left(1 + c \cdot \frac{V_t - V_{tar}}{V_{cd} - V_d}\right) \quad (5)$$

where c is a parameter calibrated to the reservoir operation data. Daily target releases and target storages, Q_{tar} and V_{tar}, are derived as the 10-day rolling mean of the multi-year median (multi-year mean) daily in situ releases and storages for within-year reservoirs (over-year reservoirs), respectively. More details on the operation scheme can be found in Dong et al. [20–22].

2.3.2. Hydropower Optimized Operation Scheme for Ideal Cases

In this study, a hydropower optimization model is also developed and coupled into the CLHMS model in order to quantitatively evaluate the best possible energy security condition of the YRB. For the five mainstream reservoirs, the objective function f is expressed as follows:

$$f = \max \sum_{t=1}^{T} g_t \cdot \Delta t \tag{6}$$

with

$$g_t(V_t, Q_t) = \gamma \left(h_t^{res} - h_t^{tail} \right) \cdot Q_t \tag{7}$$

where g_t is the hydropower output of each hydropower reservoir at the timestep t; γ is the output factor; V_t and Q_t are the reservoir storage and outflow of each reservoir at the timestep t; and h_t^{res} and h_t^{tail} are the average water level and tailwater level of each reservoir at the timestep t. Due to the fact that the reservoirs are mostly designed for hydropower generation, the flood control objective is simplified as the upper limits of the reservoir storage and outflow. These, along with the water balance and reservoir output limits, form up the constraints of the multi-timestep decision making problem, i.e.,

$$s.t. \begin{cases} V_{t+1} = V_t + (I_t - Q_t + S_t) \cdot \Delta t \\ g_{min} \le g_t(V_t, Q_t) \le g_{max} \\ V_t^{min} \le V_t \le V_t^{max} \\ Q_t^{min} \le Q_t \le Q_t^{max} \end{cases} \tag{8}$$

where V_{t+1} and V_t are the reservoir storage at the timestep $t+1$ and t, respectively; I_t and Q_t are the reservoir inflow and outflow at the timestep t, respectively; S_t is the source term in the reservoir water balance, which includes the evaporation, seepage and precipitation over the reservoir water area; and g_{min} and g_{max} are the minimum hydropower output and the hydropower storage capacity of each reservoir at the timestep t, respectively. See Section 2.3.1 for other denotations. The dynamic programming algorithm is adopted to solve the multi-timestep decision-making problem to determine the optimal release iteratively [35].

2.4. Experimental Design

To quantify the impact of water diversion and reservoir operation on the water security of the YRB, three simulation experiments were established, namely 'Natural flow', 'Reservoir' and 'Reservoir and Diversion', with a detailed workflow shown in Figure 2. A 15-year simulation (2001–2015) is conducted for each scenario. The Natural flow scenario refers to the hydrological simulation by using the CLHMS model with no account of reservoirs and water diversion, representing the natural hydrologic conditions of the YRB. The Reservoir scenario refers to the hydrologic simulation created by using the CLHMS model with reservoir operation, and represents the hydrologic conditions of the YRB under the individual impacts of reservoir operation. The Reservoir and Diversion scenario employs the CLHMS model with both water diversion and reservoir operation, in order to represent the flow regimes of the YRB under the combined impact of water diversion and reservoir operation.

Despite a dozen more hydropower reservoirs being constructed and planned in the mainstream, none of them are designed for streamflow regulation at daily scales due to their small capacity. Therefore, the five mainstream reservoirs and ten tributary reservoirs included in this study are expected to mostly represent the effect of damming on the flow regime of the YRB in the near future. That being said, the Reservoir scenario can be assumed to represent the human impact on the hydrologic regime of the YRB for the period from the full operation of the Lianghekou Reservoir (expected in 2024) to the completion of the water diversion project (no exact date so far); in addition, the Reservoir and Diversion scenario is expected to reflect the human impact on the hydrologic regime of the YRB after the completion of the water diversion project.

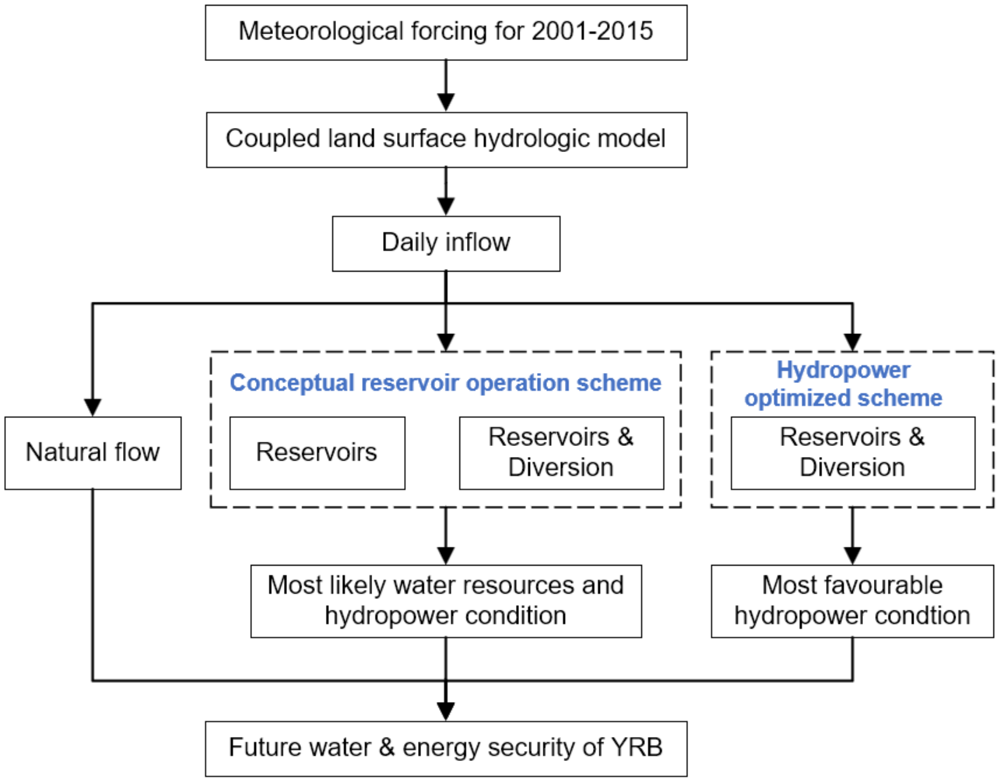

Figure 2. A general workflow of experimental design.

To investigate the impacts of water diversion and reservoir operation on the energy security of the YRB, the electricity output of the five mainstream hydropower reservoirs is calculated based on the simulated reservoir outflow and storage, and are compared between the Reservoir scenario and the Reservoir and Diversion scenario, respectively. With the conceptual reservoir operation scheme, the electricity output calculated from the Reservoir and Diversion scenario is most likely to reflect the reality after the completion of water diversion (i.e., the most likely hydropower condition). Then, we perform an additional simulation within the Reservoir and Diversion scenario by applying the optimized operation scheme to the five mainstream hydropower reservoirs, respectively, in order to investigate the largest hydropower output of the YRB (i.e., the most favorable hydropower condition) under the impact of the water diversion.

All of these simulations are carried out based on the historical climatic conditions for the period of 2001–2015.

3. Model Calibration and Validation

3.1. Reservoir Operation Simulations Calibrated to Historic Operation Data

To precisely simulate the reservoir operation and its impacts downstream, we calibrate and validate the parameters Q_{min}, Q_s, and r in the D22 conceptual reservoir operation scheme for the Ertan Reservoir and Jinping I Reservoir using the historic operation data (inflow, outflow, and storage). For the Jinping I Reservoir, we select 2014–2016 for calibration and 2017–2018 for validation. For the Ertan Reservoir, we select 2010–2016 as the calibration period and 2017–2018 as the validation period. A million parameter sets are generated randomly for the reservoir scheme, and the parameter set that gives the maximum average daily Nash–Sutcliffe Efficiency (NSE) value of the simulated storage and simulated outflow is chosen as the best one.

We present the simulated daily release and storage of the two reservoirs, respectively, in comparison with the observations in Figure 3. For the Jinping I Reservoir, the accuracy of the operation simulation is rather satisfactory for the conceptual operation scheme, with a daily NSE value of 0.90 over the entire period. For the Ertan Reservoir, the daily NSE value over the entire period is 0.84, and the NSE in the validation period (0.83) is not much lower than that in the calibration period (0.86). The root-mean square error (RMSE) is also analyzed, and the results show that the daily RMSE values of the simulated storage and simulated release are 3.5×10^8 m^3 and 544 m^3/s for the Ertan Reservoir, and are 2.8×10^8 m^3 and 268 m^3/s for the Jinping I Reservoir over the entire period. This suggests that the D22 conceptual reservoir operation scheme with calibrated parameters is generally able to represent the reservoir operation with a satisfactory accuracy.

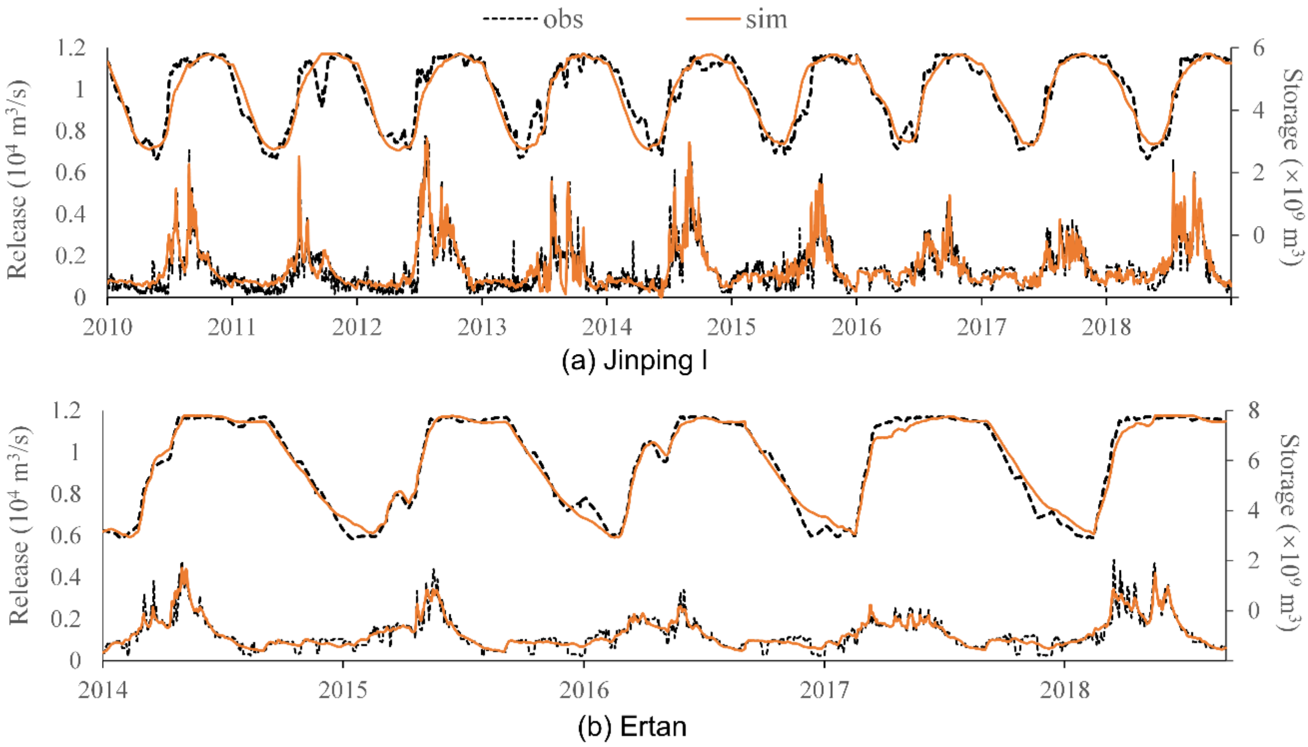

Figure 3. Daily observed and simulated release and storage of the (**a**) Ertan Reservoir and (**b**) Jinping I Reservoir using the conceptual reservoir operation scheme calibrated to historic operation data.

3.2. Reservoir Operation Simulations with Empirical Parameters

In this section, we use the conceptual reservoir operation scheme with empirical default parameters to represent the operation of the Lianghekou Reservoir, three diversion reservoirs and ten tributary reservoirs. This is because the Lianghekou Reservoir and three diversion reservoirs have not been in operation or completed, and there are no gauge records available to support the calibration procedure. The operation data of the ten tributary reservoirs are also ungauged or not made available.

The parameters Q_{min}, Q_s, and r of the D22 reservoir operation scheme are derived empirically for the Lianghekou, diversion reservoirs and tributary reservoirs. To assess the validity of empirical parameters in simulating the operation of ungauged reservoirs, here we use the empirical parameters and carry out an evaluation with respect to the Ertan Reservoir and Jinping I Reservoir. Note that the observed outflow and storage are not used to perform calibration, instead they are used for evaluation purposes only.

The simulated water storage and release of Jinping I is shown in Figure 4. For the Ertan Reservoir, the D22 reservoir operation scheme with empirical parameters can generally reconstruct the variation in its water storage, with the average NSE values of both the simulated outflow and storage being higher than 0.7. This is similar for the Jinping I

Reservoir, as the conceptual reservoir operation scheme with empirical parameters can generally reconstruct the reservoir operation processes well, with a daily NSE of 0.92 for water storage and 0.7 for reservoir outflow. In addition, the daily RMSE values of the simulated storage and simulated release are 5.9 × 10^8 m^3 and 559 m^3/s for the Ertan Reservoir, and are 5.0 × 10^8 m^3 and 474 m^3/s for the Jinping I Reservoir over the entire period. These results reveal the applicability of the D22 reservoir operation scheme to simulate the reservoir operation of ungauged reservoirs in the YRB, suggesting that the D22 reservoir operation scheme has the potential to reasonably reconstruct the reservoir operation processes without historic operation records.

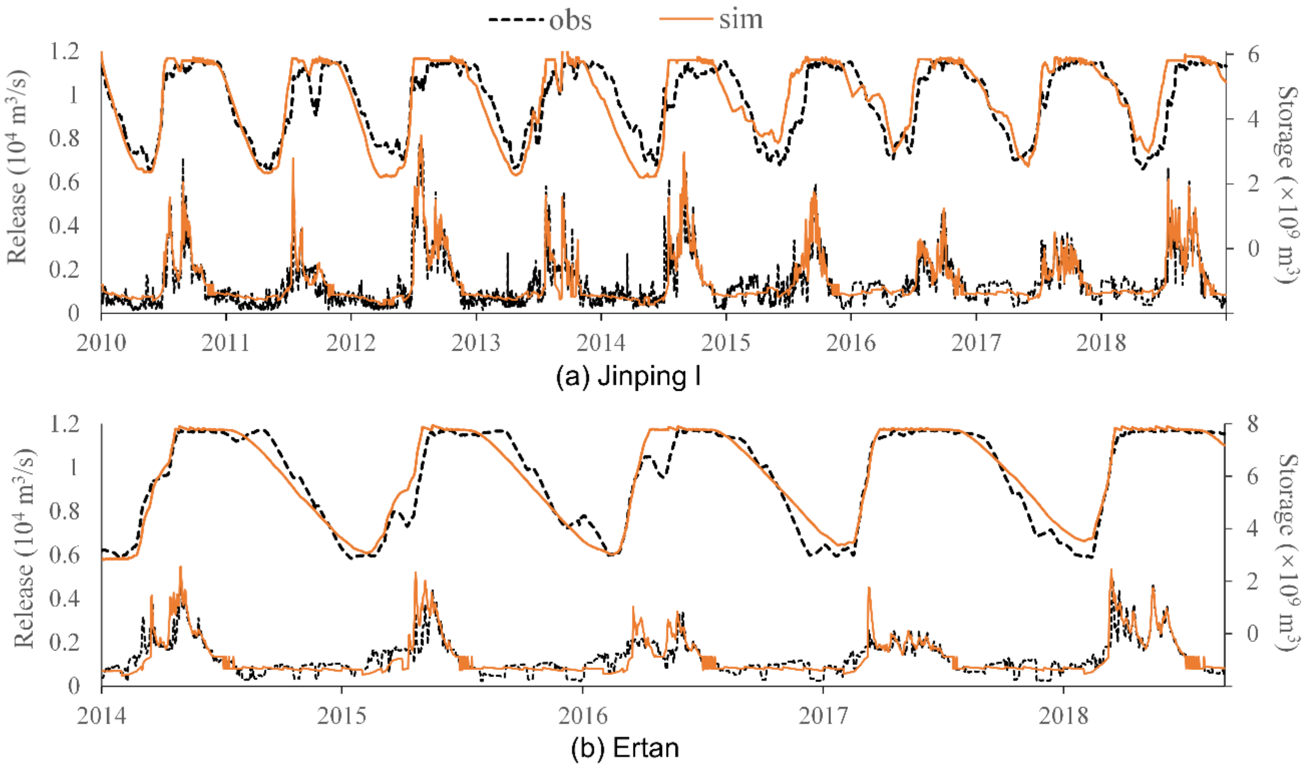

Figure 4. The daily observed and simulated outflow and storage of the (**a**) Ertan Reservoir and (**b**) Jinping I Reservoir using the conceptual reservoir operation scheme with empirical parameters.

In general, the employed reservoir operation scheme exhibits a fairly satisfactory accuracy in reconstructing observed reservoir release and storage in the YRB. However, the employed reservoir operation scheme is nevertheless a simplification of actual reservoir operation. Real-time decision making on dam releases usually takes account of streamflow forecasts, fluctuating water demands, and manual experiences, which can induce uncertainties in the simulation of reservoir operation. These uncertainties should be further investigated in future studies.

3.3. Gauge-Based Streamflow Calibration and Validation of the CLHMS Model

In this section, the CLHMS model, without reservoir operation schemes, is calibrated to the daily observed streamflow of the Yajiang and Ertan hydrologic stations. The calibration periods are selected to be 2006–2008 and 2001–2010, respectively, to avoid the impact of upstream reservoir operation on the hydrologic regime, since the reservoirs upstream of these stations were generally not built until the 2010s. For each station, 1000 parameter sets are sampled using the Latin Hypercube [36], and the parameter sets with the highest NSE are chosen as the optimal set. LHS is a stratified sampling technique, in which the distribution of each parameter is divided into strata of equal probability [37].

Figure 5 presents the calibration and validation results with the relative bias (RB) and the daily NSE. It shows that the performance of the CLHMS model without reservoirs is fairly good, and that most of the NSE values are higher than 0.80. Notably, the NSE in the validation period of 2011–2015 at Ertan (0.64) is lower than that in the calibration period of 2001–2010 (0.86). This could be a result of the reservoir construction upstream of the Ertan station during the validation period; reservoir operation could significantly alter the hydrologic regime, which cannot be accurately depicted by the CLHMS model without reservoir representations.

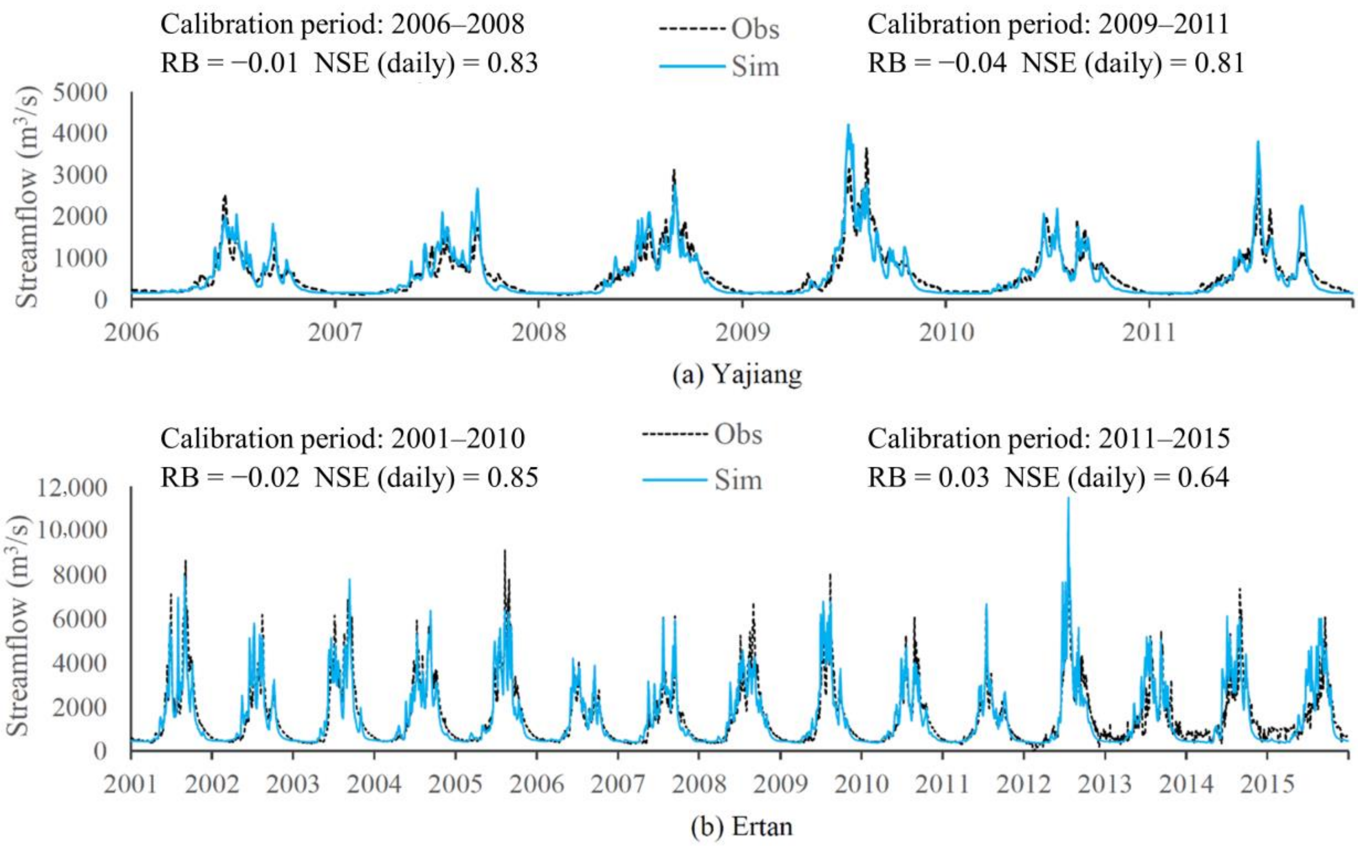

Figure 5. The simulated and observed daily streamflow at (**a**) Yajiang and (**b**) Ertan.

To investigate whether the decreased model performance in the validation period is mainly caused by the lack of representations of reservoir operation in the model, an additional model run is performed by representing the reservoir operation using the conceptual reservoir operation scheme with calibrated parameters for the Jinping I and Ertan, and with empirical parameters for the Lianghekou and tributary reservoirs. The simulated streamflow at Ertan with and without reservoir consideration in the CLHMS model is shown in Figure 6. Note that the reservoir in the model is activated only after the model reaches the time point at which that reservoir was put into full operation in reality. It means, for example, that the Jinping I Reservoir was deactivated until 2013 and the Lianghekou Reservoir was never activated during the calibration and validation period of the model. In general, it is found that coupling reservoirs to the hydrologic model using the reservoir operation scheme can improve the model performance in the river flow simulation during the validation period, as the daily NSE at Ertan is increased from 0.64 to 0.81 during this period. This indicates that, in addition to reproducing the dynamics of the selected reservoirs in the basin well, the CLHMS model with the reservoir operation scheme can serve as a reliable tool to understand the hydrological impact of reservoirs.

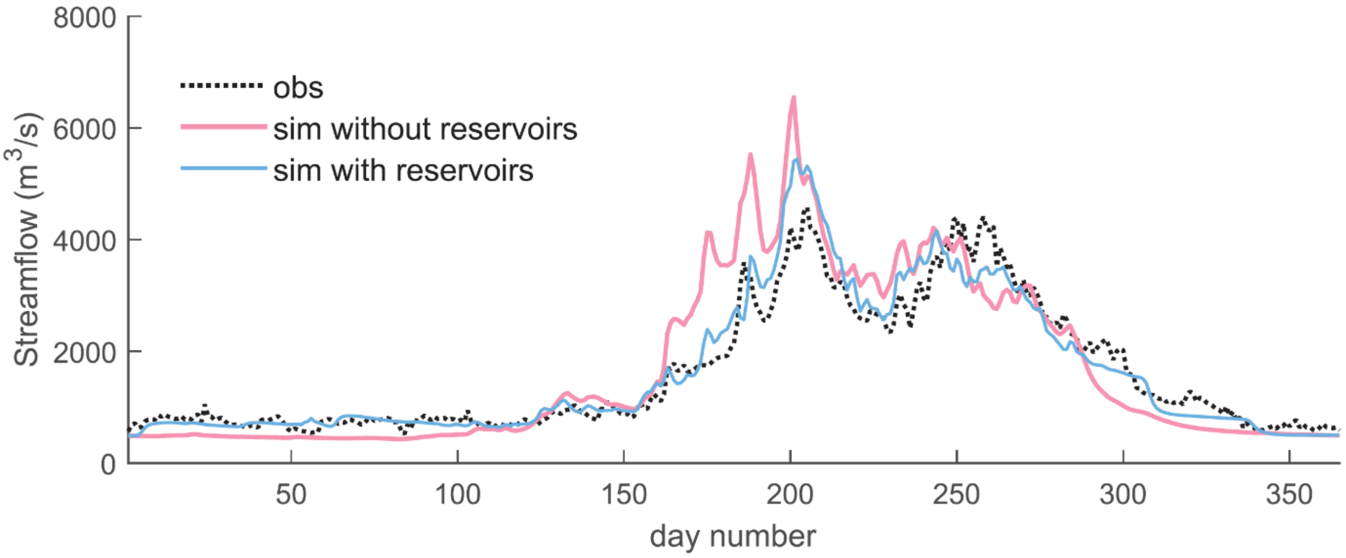

Figure 6. The daily observed and simulated streamflow at Ertan averaged over the validation period before and after integrating reservoirs with the conceptual reservoir operation scheme in the CLHMS model.

4. Impacts of Reservoir Operation and Water Diversion

4.1. Water Resources under Reservoir Operation

In Figure 7, the monthly streamflow at the Ertan station is depicted along with its differences under the Natural flow scenario, the Reservoirs scenario, and the Reservoir and Diversion scenario. For the Reservoir scenario, reservoir operation can greatly reduce the variation in the streamflow during a seasonal cycle. The wet season (June to October) sees 19% less streamflow (540 m^3/s) (19%), and the dry season (November to May) experiences 66% more streamflow (435 m^3/s). The monthly streamflow variation during annual cycles is also reduced, and the monthly streamflow interval within the 10% and 90% percentile is reduced from ~850 m^3/s to ~550 m^3/s, averaged over a year. This is especially the case for streamflow in the wet season, where the average 10–90 interval is reduced from ~1700 m^3/s to ~1100 m^3/s.

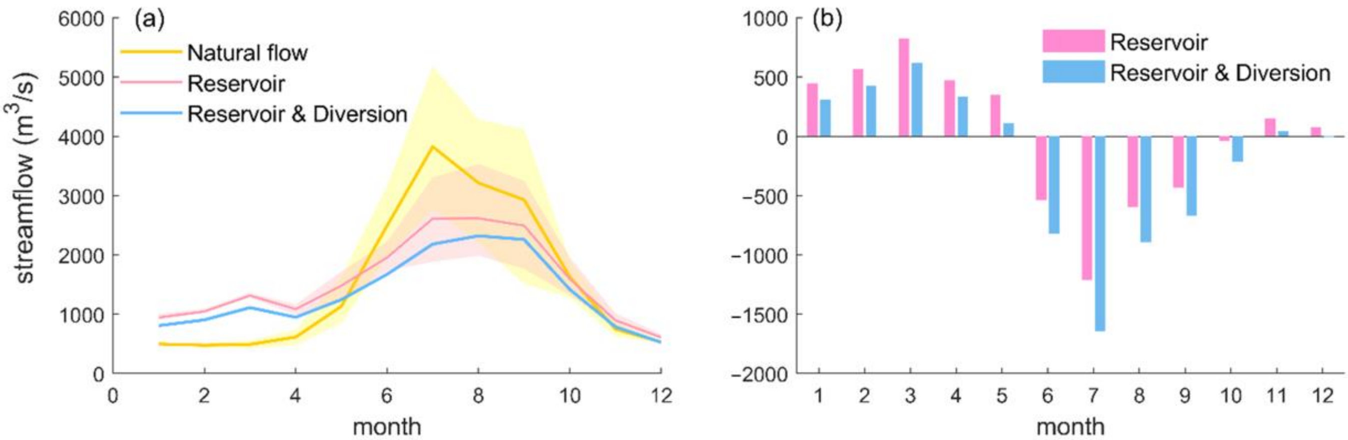

Figure 7. (**a**) Monthly simulated streamflow at the Ertan station and (**b**) its difference under the Reservoir scenario and the Reservoir and Diversion scenario, in comparison to the natural flow regime averaged over the study period. The shaded area denotes the 10–90 percentile interval.

Figure 8 depicts the streamflow variations induced by reservoirs during the dry season and the wet season, respectively, at the grid cell scale. Individual tributary reservoirs are mostly located upstream of a river and can have a major impact on the local flow regimes, for instance the Buxi Reservoir can decrease the wet season river discharge by 9% (Figure 8a) and increase the dry season river discharge by over 200% (Figure 8b). However, the impact of a single reservoir in the tributary rapidly weakens towards the downstream areas due to the incoming lateral flow. On the other hand, the reservoirs in the mainstream are able to effectively modulate the downstream flow regimes, especially for the Lianghekou Reservoir, which reduces the streamflow for the wet season by 281m^3/s (32%) and increases the streamflow for the dry season by 291 m^3/s (118%). For the most downstream reservoir of the YRB, the downstream river discharge of the Ertan Reservoir is 507 m^3/s (79%) higher in the dry season and 659 m^3/s (23%) lower in the wet season than the natural flow scenario.

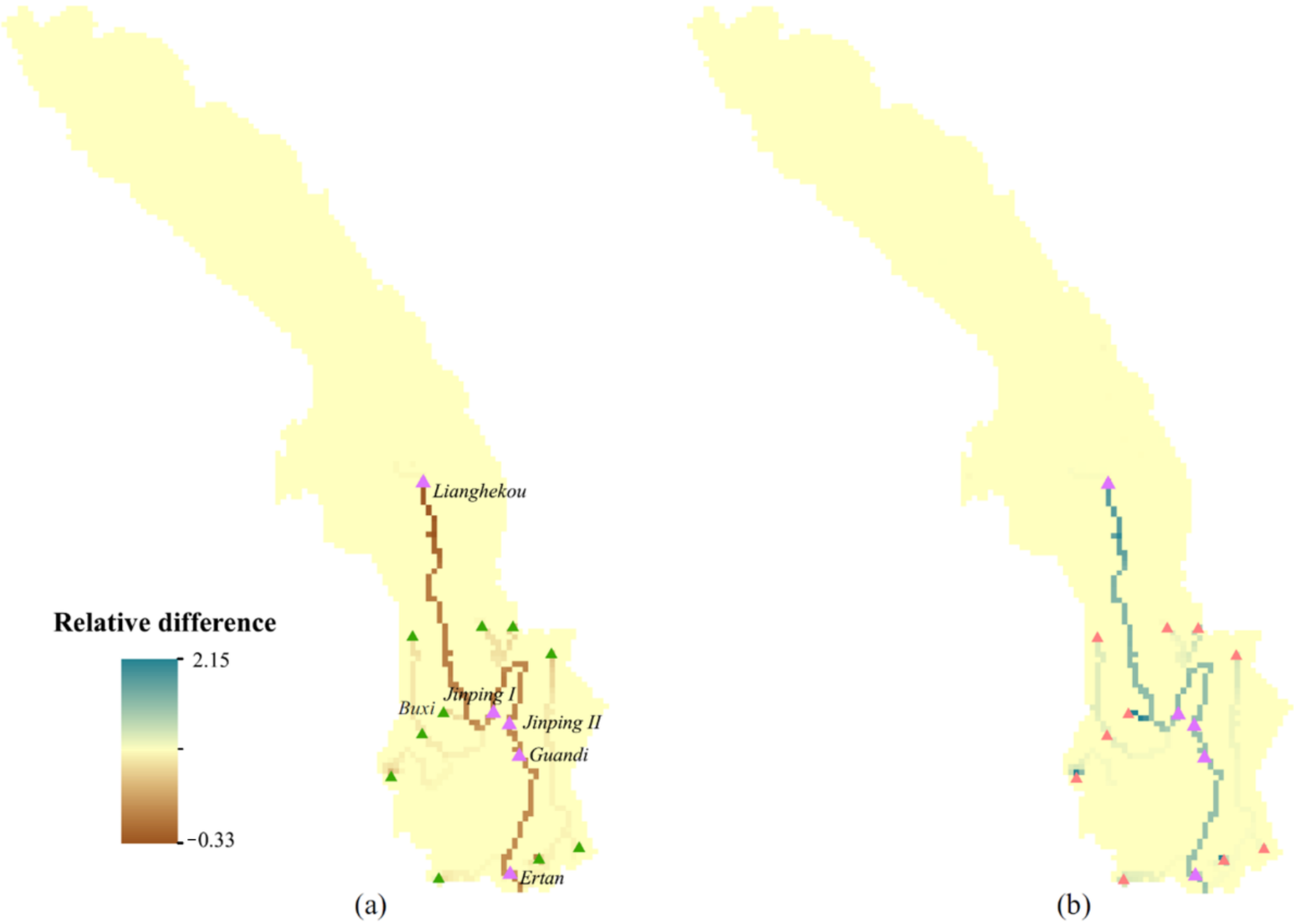

Figure 8. The relative difference in the monthly streamflow (**a**) for the wet season and (**b**) for the dry season between the Reservoir scenario and the Natural flow scenario, averaged over the study period of 2001–2015. Triangles denote reservoirs, see the legend of Figure 1 for details.

4.2. Water Resources under Water Diversion and Reservoir Operation

As also indicated in Figure 7a, in comparison with the Natural flow scenario, the monthly streamflow under the Reservoir and Diversion scenario is 823 m^3/s (29%) lower for the wet season and 233 m^3/s (36%) higher for the dry season despite a large amount of diverted water in the dry season. In comparison with the Reservoir scenario, on the other hand, the monthly streamflow under the Reservoir and Diversion scenario sees an average decrease of 10–20% for all months (Figure 7b).

Figure 9 depicts the spatial distribution of streamflow variations in the dry and wet seasons under the Reservoir and Diversion scenario compared to the Natural flow scenario.

For the dry season (Figure 9a), the monthly streamflow is decreased by 30–60% immediately downstream of Reba, Aan, and Renda due to water diversion. The Lianghekou Reservoir along the mainstream alone could offset the diverted water loss in the dry season, as the release of Lianghekou, Jinping I and Ertan in the dry season is 38%, 43% and 50% higher than the Natural flow scenario, respectively. For the wet season (Figure 9b), the monthly streamflow is reduced by 18–33% immediately downstream of Reba, Aan, and Renda compared to the Natural flow scenario. The Lianghekou, Jinping I and Ertan Reservoir further reduces the streamflow in the wet season by 53%, 34% and 32% compared to the Natural flow scenario, respectively.

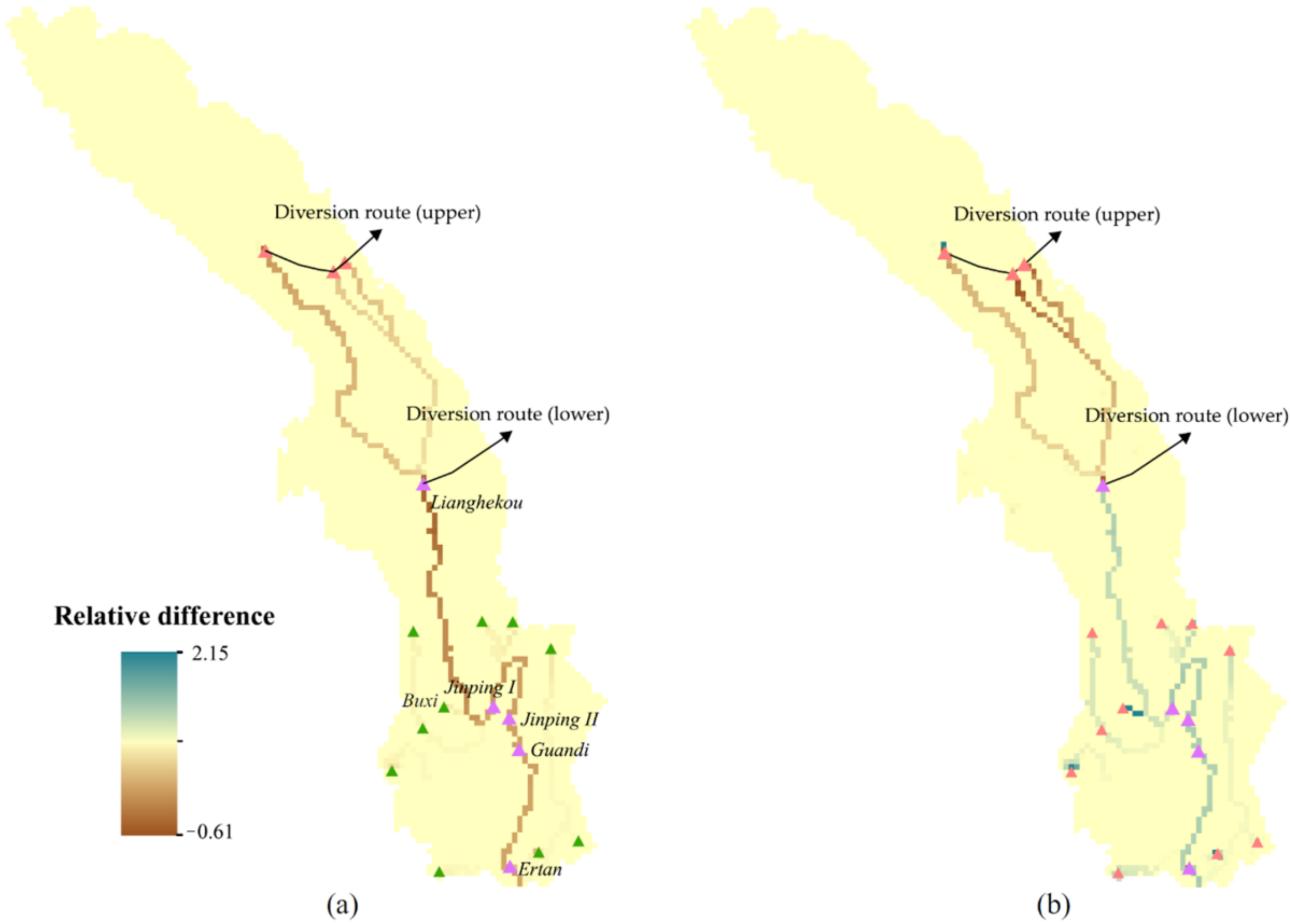

Figure 9. The relative difference in the monthly streamflow (**a**) for the wet season and (**b**) for the dry season between the Reservoir and Diversion scenario and the Natural flow scenario, averaged over the simulation period. Triangles denote reservoirs, see the legend of Figure 1 for details.

4.3. Hydropower Output under Water Diversion and Reservoir Operation

The impact of water diversion on the hydropower output of the five mainstream hydropower reservoirs is quantified through a comparative analysis between the Reservoir scenario and the Reservoir and Diversion scenario. As can be seen in Figure 10, the average total hydropower output of the five hydropower reservoirs is 901×10^8 kW·h per year without the water diversion, and is likely to reduce by 16% to 748×10^8 kW·h per year with the water diversion. To be specific, the hydropower output of Lianghekou, Jinping I, Jinping II, Guandi, and Ertan is reduced by 34%, 19%, 12%, 13% and 13%, respectively. The upstream reservoirs, e.g., the Lianghekou Reservoir, generally experience a relatively larger decrease in the hydropower output than the downstream reservoirs, as they are closer to the water diversion and suffer a larger impact in terms of the water lost to diversion.

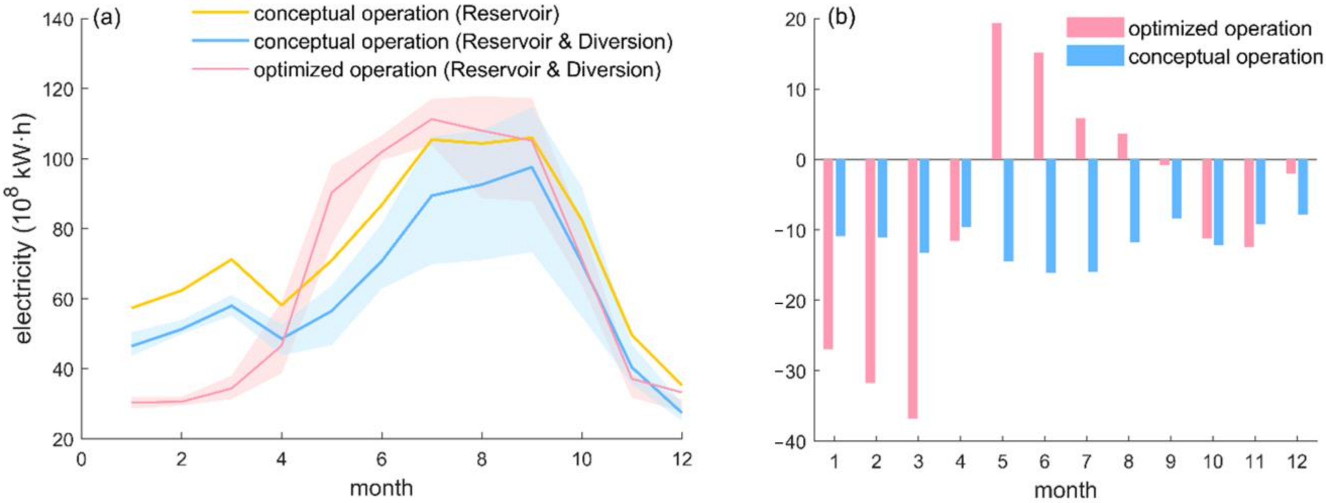

Figure 10. (**a**) The average total hydropower output (kW·h) of the five hydropower reservoirs under the Reservoir scenario and the Reservoir and Diversion scenario, and (**b**) the sole impact of water diversion on the hydropower output (kW·h) with the conceptual scheme and the hydropower optimization model. The shaded area denotes the 10–90 percentile interval.

To further investigate the maximum possible hydropower output under the impact of water diversion, the reservoir optimization model, with maximizing the hydropower output as the objective function (Section 2.3.2), is applied to each reservoir under the Reservoir and Diversion scenario (Figure 10). The results indicate that, with the hydropower optimization model, the average total hydropower output of the five hydropower reservoirs under the impact of water diversion is 808 $\times$ 10^8 kW·h per year, an 8% or approximately 60 $\times$ 10^8 kW·h increase per year relative to the conceptual reservoir operation. The Lianghekou, Jinping I, Jinping II, Guandi, and Ertan Reservoir, with the optimized operation scheme, experience a 7 $\times$ 10^8 kW·h (10%), 31 $\times$ 10^8 kW·h (20%), 0%, 0%, and 20 $\times$ 10^8 kW·h (12%) increase per year in the hydropower output compared to the conceptual reservoir operation scheme, respectively. Temporally, the optimized hydropower output sees a notable increase from May to August but a decrease from January to March, compared to the conceptual reservoir operation scheme, leading to a larger discrepancy in the energy output among seasons.

5. Discussion

5.1. Implications for Water Security and Ecological Security

The Yalong River Basin has been under extensive hydropower development in the past ten years, and the revised western route of the South-to-North Water Diversion Project could further complicate the hydrologic conditions in the major tributary of the Yangtze River. Our gauge and spatial results (Figures 7 and 8) highlight the role of reservoirs in remarkably alleviating the temporal and spatial variability in water resources in the basin, which leads to the improved water security of the basin, especially along the mainstream. The prominent increase in the dry season streamflow relative to the natural conditions can bring many benefits to local water-dependent industries and to aquatic communities that are sensitive to the baseflow [38]. This is especially relevant for the dominant local species, *Schizothorax chongi*, which takes the downstream area of Jinping I as a major spawning area and relies on the streamflow during April and May to spawn [39]. Compared to the natural conditions, the streamflow in April and May would see a large increase under reservoir operation (Figure 7), which could create a favorable hydrologic condition for them to locate a spawning area (see Li et al. [40] for more details on the ecological conservation levels for *Schizothorax chongi*). However, reservoirs can also bring about several ecological disadvantages, as the notable decline of the high flows and flow variability are unfavorable to the transfer of nutrient and organic substances, and may entrap organisms on the islands and floodplains [41].

The updated West Route water diversion can impact the flow regime of the YRB especially in regions above the Lianghekou Reservoir (Figure 9). The diversion reservoirs serve to keep a balance of water resources between the dry season and wet season as much as possible, but are unlikely to fully restore the streamflow in the dry season back to the natural conditions. The decrease in the streamflow would nevertheless cause a drop in the water level and water area, and may result in wetland degradation and species decline upstream of the Lianghekou Reservoir, albeit a much less ecological impact compared to the previous version of the diversion scheme in which a doubled water volume is designed for diversion. Therefore, ecological preservation measures may be necessary to address the potential threats that the water diversion poses to the aquatic environment and biodiversity along this river section. The socioeconomic development, on the other hand, is unlikely to be affected, given that the areas upstream of the Lianghekou Reservoir are very sparsely populated due to its relatively uninhabitable environment. For areas downstream of the Lianghekou Reservoir, an overall improved water security is expected, as the reservoir operation could mitigate the effect of water diversion on the streamflow in the dry season by increasing the streamflow to a level much higher than that in the natural conditions. The streamflow in the wet season can be further reduced, which could bring benefits to flood control along the lower mainstream and further downstream areas.

5.2. Implications for Energy Security

In terms of the hydropower generation, a less desirable energy output is expected in the future under the impact of water diversion, primarily because of the decrease in the reservoir inflow. Notably, reservoir operation with the optimized scheme can produce approximately 8% more energy than the conceptual reservoir operation scheme, despite a larger discrepancy among seasons (Figure 10).

Here, we further analyze the outflow and storage of the Ertan Reservoir to investigate the cause of the increase in the energy output with the optimized scheme relative to the conceptual one. It is found that Ertan is operated to maintain a higher water level and a large gravity head throughout the year in order to achieve the maximum hydropower generation, and other reservoirs generally show a similar pattern to Ertan. However, such a strategy results in a small release in the dry season, which causes the energy output in the dry season to significantly decline compared to the conceptual operation. This could contradict the timing of the electricity demand because of the potential high electricity loads in the winter. Nevertheless, given the 8% increase with the optimized scheme, there is hydropower potential yet to be exploited to further meet the rapidly growing energy demand in the southwestern China; this is only if the current issues, for example, the uncertainties of the incoming flow for reservoir optimization, can be addressed well in the real-time reservoir operation.

Our finding also suggests that adapting the operation schemes alone may not be able to compensate for the diversion-induced decrease in the energy output, because even the optimized reservoir operation rules could not produce as much electricity as without the water diversion. Therefore, back-up plans and long-term considerations may be necessary to cope with the anticipated decline in the hydropower output in the future in order to achieve more clean energy and ultimately an environmentally friendly society [42,43].

6. Conclusions

In this study, we employ a hydrological modelling framework that couples a land surface–hydrologic model with reservoir operation modules to allow quantifying the hydrologic impact of reservoir operation and water diversion. The coupled CLHMS model is applied to the Yalong River Basin in China where several large-sized reservoirs and the western route of the South-to-North Water Diversion project are under construction and planning. Four 15-year (2001–2015) simulations, with a spatial resolution of 5 km, were conducted to analyze the likely streamflow variations under different water resource management scenarios, and to investigate the most likely and the most favorable hydropower condition of the major hydropower reservoirs in the YRB under the future impact of the dam operation and water diversion. Major conclusions are highlighted as follows.

Reservoirs across the YRB are able to effectively modulate the flow regimes by reducing the peak flows in the wet season and increasing the low flows in the dry season for enhanced water security conditions of the basin. With the further impact of water diversion, the river section between the diversion reservoirs and the Lianghekou reservoir is expected to experience a relatively large decrease in the streamflow in both dry and wet seasons, in comparison with the natural condition; this calls for preservation measures in the ecosystem. For areas downstream of the Lianghekou Reservoir, the diversion-induced decline in the streamflow in the dry season is likely to be fully mitigated by reservoir operation, as the streamflow in the dry season can be increased to a level 38–51% higher than the natural flow conditions. The streamflow in the wet season can be further reduced, which could benefit the flood control further downstream.

The hydropower output is over 900 kW·h per year for the five mainstream hydropower reservoirs after the full operation of Lianghekou; this is likely to decrease by 16% with the current conceptual reservoir operation scheme and decrease by 10% with the hydropower-optimized operation scheme under the impact of reservoir operation and water diversion. The adaption of current operation rules alone may not be able to reverse the decline in the energy production, calling for additional adaption measures to deal with the anticipated decline in the hydropower output.

Overall, our presented modeling framework provides insight into the water and energy security of the YRB by depicting, as realistically as possible, the impact of anthropogenic activities on the terrestrial water system in a fully coupled land surface–hydrologic model; this can be applied further downstream to the Yangtze River and in different regions worldwide. Future work includes improving the reservoir operation simulations of ungauged reservoirs with remote sensing techniques.

Author Contributions: Methodology, J.X. and N.D. All authors have read and agreed to the published version of the manuscript.

Funding: This work was funded by the Open Research Fund of Key Laboratory of Flood & Drought Disaster Defense, the Ministry of Water Resources, Grant NO. KYFB202112071051.

Institutional Review Board Statement: Not applicable.

Informed Consent Statement: Not applicable.

Data Availability Statement: Reservoir operation data is available from the corresponding author.

Conflicts of Interest: The authors declare no conflict of interest.

References

1. Liu, J.; Yang, H.; Gosling, S.N.; Kummu, M.; Flörke, M.; Pfister, S.; Hanasaki, N.; Wada, Y.; Zhang, X.; Zheng, C.; et al. Water scarcity assessments in the past, present, and future. *Earth's Future* **2017**, *5*, 545–559. [CrossRef] [PubMed]
2. Boulange, J.; Hanasaki, N.; Yamazaki, D.; Pokhrel, Y. Role of dams in reducing global flood exposure under climate change. *Nat. Commun.* **2021**, *12*, 1–7. [CrossRef] [PubMed]
3. Wada, Y.; de Graaf, I.E.; van Beek, L.P. High-resolution modeling of human and climate impacts on global water resources. *J. Adv. Model. Earth Syst.* **2016**, *8*, 735–763. [CrossRef]
4. Hanasaki, N.; Kanae, S.; Oki, T. A reservoir operation scheme for global river routing models. *J. Hydrol.* **2006**, *327*, 22–41. [CrossRef]
5. Wan, W.; Zhao, J.; Popat, E.; Herbert, C.; Döll, P. Analyzing the Impact of Streamflow Drought on Hydroelectricity Production: A Global-Scale Study. *Water Resour. Res.* **2021**, *57*, e2020WR028087. [CrossRef]
6. Wada, Y.; van Beek, L.P.H.; Bierkens, M.F.P. Modelling global water stress of the recent past: On the relative importance of trends in water demand and climate variability. *Hydrol. Earth Syst. Sci.* **2011**, *15*, 3785–3808. [CrossRef]
7. Wada, Y.; Bierkens, M.F.P.; de Roo, A.; Dirmeyer, P.A.; Famiglietti, J.S.; Hanasaki, N.; Konar, M.; Liu, J.; Schmied, H.M.; Oki, T.; et al. Human–water interface in hydrological modelling: Current status and future directions. *Hydrol. Earth Syst. Sci.* **2017**, *21*, 4169–4193. [CrossRef]

8. Räsänen, T.A.; Someth, P.; Lauri, H.; Koponen, J.; Sarkkula, J.; Kummu, M. Observed river discharge changes due to hydropower operations in the Upper Mekong Basin. *J. Hydrol.* **2017**, *545*, 28–41. [CrossRef]
9. Wang, Y.; Li, J.; Zhang, T.; Wang, B. Changes in drought propagation under the regulation of reservoirs and water diversion. *Theor. Appl. Clim.* **2019**, *138*, 701–711. [CrossRef]
10. Zhao, G.; Gao, H.; Naz, B.S.; Kao, S.-C.; Voisin, N. Integrating a reservoir regulation scheme into a spatially distributed hydrological model. *Adv. Water Resour.* **2016**, *98*, 16–31. [CrossRef]
11. Ehsani, N.; Vörösmarty, C.J.; Fekete, B.M.; Stakhiv, E.Z. Reservoir operations under climate change: Storage capacity options to mitigate risk. *J. Hydrol.* **2017**, *555*, 435–446. [CrossRef]
12. Hanasaki, N.; Yoshikawa, S.; Pokhrel, Y.; Kanae, S. A global hydrological simulation to specify the sources of water used by humans. *Hydrol. Earth Syst. Sci.* **2018**, *22*, 789–817. [CrossRef]
13. Wisser, D.; Fekete, B.M.; Vörösmarty, C.J.; Schumann, A.H. Reconstructing 20th century global hydrography: A contribution to the Global Terrestrial Network- Hydrology (GTN-H). *Hydrol. Earth Syst. Sci.* **2010**, *14*, 1–24. [CrossRef]
14. Arheimer, B.; Donnelly, C.; Lindström, G. Regulation of snow-fed rivers affects flow regimes more than climate change. *Nat. Commun.* **2017**, *8*, 1–9. [CrossRef]
15. Clark, M.P.; Zolfaghari, R.; Green, K.R.; Trim, S.; Knoben, W.J.M.; Bennett, A.; Nijssen, B.; Ireson, A.; Spiteri, R.J. The numerical implementation of land models: Problem formulation and laugh tests. *J. Hydrometeorol.* **2021**, *22*, 1627–1648. [CrossRef]
16. Fleischmann, A.; Brêda, J.; Passaia, O.; Wongchuig, S.; Fan, F.; Paiva, R.; Marques, G.; Collischonn, W. Regional scale hydrodynamic modeling of the river-floodplain-reservoir continuum. *J. Hydrol.* **2021**, *596*, 126114. [CrossRef]
17. Akter, A.; Babel, M.S. Hydrological modeling of the Mun River basin in Thailand. *J. Hydrol.* **2012**, *452*, 232–246. [CrossRef]
18. Hoang, L.P.; van Vliet, M.T.; Kummu, M.; Lauri, H.; Koponen, J.; Supit, I.; Leemans, R.; Kabat, P.; Ludwig, F. The Mekong's future flows under multiple drivers: How climate change, hydropower developments and irrigation expansions drive hydrological changes. *Sci. Total. Environ.* **2019**, *649*, 601–609. [CrossRef]
19. Lu, Z.; Feng, Q.; Xiao, S.; Xie, J.; Zou, S.; Yang, Q.; Si, J. The impacts of the ecological water diversion project on the ecology-hydrology-economy nexus in the lower reaches in an inland river basin. *Resour. Conserv. Recycl.* **2021**, *164*, 105154. [CrossRef]
20. Dong, N.; Wei, J.; Yang, M.; Yan, D.; Yang, C.; Gao, H.; Arnault, J.; Laux, P.; Zhang, X.; Liu, Y.; et al. Model Estimates of China's Terrestrial Water Storage Variation Due To Reservoir Operation. *Water Resour. Res.* **2022**, *58*, e2021WR031787. [CrossRef]
21. Dong, N.; Yang, M.; Wei, J.; Arnault, J.; Laux, P.; Xu, S.; Wang, H.; Yu, Z.; Kunstmann, H. Towards improved parameterizations of reservoir operation in ungauged basins: A synergistic framework coupling satellite remote sensing, hydrologic modeling and conceptual operation schemes. *Water Resour. Res.* **2023**, e2022WR033026. [CrossRef]
22. Dong, N.; Guan, W.; Cao, J.; Zou, Y.; Yang, M.; Wei, J.; Chen, L.; Wang, H. A hybrid hydrologic modelling framework with data-driven and conceptual reservoir operation schemes for reservoir impact assessment and predictions. *J. Hydrol.* **2023**, *619*, 129246. [CrossRef]
23. Celeste, A.B.; Billib, M. The Role of Spill and Evaporation in Reservoir Optimization Models. *Water Resour. Manag.* **2009**, *24*, 617–628. [CrossRef]
24. Mamede, G.L.; Guentner, A.; Medeiros, P.H.A.; de Araújo, J.C.; Bronstert, A. Modeling the Effect of Multiple Reservoirs on Water and Sediment Dynamics in a Semiarid Catchment in Brazil. *J. Hydrol. Eng.* **2018**, *23*, 05018020. [CrossRef]
25. Gu, H.; Yu, Z.; Yang, C.; Ju, Q. Projected Changes in Hydrological Extremes in the Yangtze River Basin with an Ensemble of Regional Climate Simulations. *Water* **2018**, *10*, 1279. [CrossRef]
26. Liu, X.; Yang, M.; Meng, X.; Wen, F.; Sun, G. Assessing the Impact of Reservoir Parameters on Runoff in the Yalong River Basin using the SWAT Model. *Water* **2019**, *11*, 643. [CrossRef]
27. Xu, A. The Upper and the Lower Route of the West Route of South-to-North Diversion Are Envisaged. 2021. Available online: http://lw.xinhuanet.com/2021-03/29/c_139844105.htm (accessed on 29 March 2021). (In Chinese).
28. Yu, Z.; Lakhtakia, M.; Yarnal, B.; White, R.; Miller, D.; Frakes, B.; Barron, E.; Duffy, C.; Schwartz, F. Simulating the river-basin response to atmospheric forcing by linking a mesoscale meteorological model and hydrologic model system. *J. Hydrol.* **1999**, *218*, 72–91. [CrossRef]
29. Yu, Z.; Pollard, D.; Cheng, L. On continental-scale hydrologic simulations with a coupled hydrologic model. *J. Hydrol.* **2006**, *331*, 110–124. [CrossRef]
30. Wagner, S.; Fersch, B.; Yuan, F.; Yu, Z.; Kunstmann, H. Fully coupled atmospheric-hydrological modeling at regional and long-term scales: Development, application, and analysis ofWRF-HMS. *Water Resour. Res.* **2016**, *52*, 3187–3211. [CrossRef]
31. Yang, C. Research on Coupling Land Surface-Hydrology Model and Application. Ph.D. Thesis, Hohai University, Nanjing, China, 2009.
32. Yang, C.; Lin, Z.; Yu, Z.; Hao, Z.; Liu, S. Analysis and Simulation of Human Activity Impact on Streamflow in the Huaihe River Basin with a Large-Scale Hydrologic Model. *J. Hydrometeorol.* **2010**, *11*, 810–821. [CrossRef]
33. Yang, C.; Yu, Z.; Hao, Z.; Zhang, J.; Zhu, J. Impact of climate change on flood and drought events in Huaihe River Basin, China. *Hydrol. Res.* **2012**, *43*, 14–22. [CrossRef]
34. Yang, C.; Yu, Z.; Hao, Z.; Lin, Z.; Wang, H. Effects of Vegetation Cover on Hydrological Processes in a Large Region: Huaihe River Basin, China. *J. Hydrol. Eng.* **2013**, *18*, 1477–1483. [CrossRef]
35. Zhao, T.; Zhao, J.; Lei, X.; Wang, X.; Wu, B. Improved Dynamic Programming for Reservoir Flood Control Operation. *Water Resour. Manag.* **2017**, *31*, 2047–2063. [CrossRef]

36. Ehlers, L.B.; Sonnenborg, T.O.; Refsgaard, J.C. Observational and predictive uncertainties for multiple variables in a spatially distributed hydrological model. *Hydrol. Process.* **2019**, *33*, 833–848. [CrossRef]
37. Mckay, M.D.; Beckman, R.J.; Conover, W.J. A Comparison of Three Methods for Selecting Values of Input Variables in the Analysis of Output from a Computer Code. *Technometrics* **1979**, *21*, 239–245.
38. Wang, Y.; Zhang, N.; Wang, D.; Wu, J.; Zhang, X. Investigating the impacts of cascade hydropower development on the natural flow regime in the Yangtze River, China. *Sci. Total. Environ.* **2018**, *624*, 1187–1194. [CrossRef]
39. Wang, Y.; Zhang, W.; Zhao, Y.; Peng, H.; Shi, Y. Modelling water quality and quantity with the influence of inter-basin water diversion projects and cascade reservoirs in the Middle-lower Hanjiang River. *J. Hydrol.* **2016**, *541*, 1348–1362. [CrossRef]
40. Li, R.; Chen, Q.; Duan, C. Ecological hydrograph based on Schizothorax chongi habitat conservation in the dewatered river channel between Jinping cascaded dams. *Sci. China Technol. Sci.* **2011**, *54*, 54–63. [CrossRef]
41. Hu, W.-W.; Wang, G.-X.; Deng, W.; Li, S.-N. The influence of dams on ecohydrological conditions in the Huaihe River basin, China. *Ecol. Eng.* **2008**, *33*, 233–241. [CrossRef]
42. O'Neill, B.C.; Oppenheimer, M.; Warren, R.; Hallegatte, S.; Kopp, R.E.; Pörtner, H.O.; Scholes, R.; Birkmann, J.; Foden, W.; Licker, R.; et al. IPCC reasons for concern regarding climate change risks. *Nat. Clim. Chang.* **2017**, *7*, 28–37. [CrossRef]
43. Zhao, Y.; Zhu, Y.; Lin, Z.; Wang, J.; He, G.; Li, H.; Li, L.; Wang, H.; Jiang, S.; He, F.; et al. Energy Reduction Effect of the South-to-North Water Diversion Project in China. *Sci. Rep.* **2017**, *7*, 1–9. [CrossRef] [PubMed]